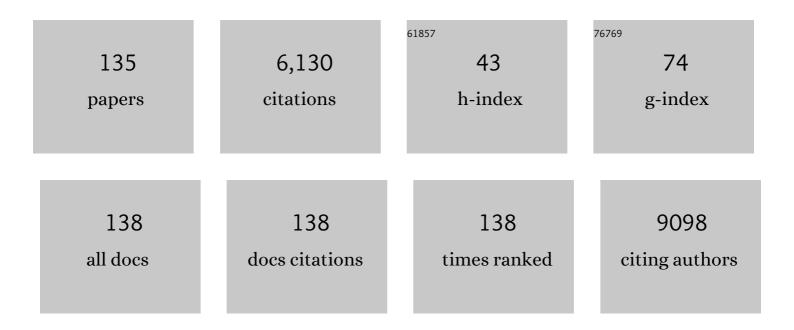
List of Publications by Year in descending order

Source: https://exaly.com/author-pdf/9306410/publications.pdf Version: 2024-02-01



SEANLI

#	Article	IF	CITATIONS
1	Phosphorus-Based Alloy Materials for Advanced Potassium-Ion Battery Anode. Journal of the American Chemical Society, 2017, 139, 3316-3319.	6.6	755
2	Atomic Interface Engineering and Electricâ€Field Effect in Ultrathin Bi ₂ MoO ₆ Nanosheets for Superior Lithium Ion Storage. Advanced Materials, 2017, 29, 1700396.	11.1	343
3	A review of Sb2Se3 photovoltaic absorber materials and thin-film solar cells. Solar Energy, 2020, 201, 227-246.	2.9	243
4	Photocatalytic solar fuel production and environmental remediation through experimental and DFT based research on CdSe-QDs-coupled P-doped-g-C3N4 composites. Applied Catalysis B: Environmental, 2020, 270, 118867.	10.8	165
5	Tuning the surface oxygen concentration of {111} surrounded ceria nanocrystals for enhanced photocatalytic activities. Nanoscale, 2016, 8, 378-387.	2.8	163
6	Synthesis of S-Doped porous g-C3N4 by using ionic liquids and subsequently coupled with Au-TiO2 for exceptional cocatalyst-free visible-light catalytic activities. Applied Catalysis B: Environmental, 2018, 237, 1082-1090.	10.8	151
7	Switching of magnetic easy-axis using crystal orientation for large perpendicular coercivity in CoFe2O4 thin film. Scientific Reports, 2016, 6, 30074.	1.6	148
8	A solution-processed TiS ₂ /organic hybrid superlattice film towards flexible thermoelectric devices. Journal of Materials Chemistry A, 2017, 5, 564-570.	5.2	130
9	Structural Insight into Layer Gliding and Lattice Distortion in Layered Manganese Oxide Electrodes for Potassiumã€ion Batteries. Advanced Energy Materials, 2019, 9, 1900568.	10.2	125
10	One-step colloid fabrication of nickel phosphides nanoplate/nickel foam hybrid electrode for high-performance asymmetric supercapacitors. Chemical Engineering Journal, 2019, 373, 1132-1143.	6.6	120
11	High-κ perovskite membranes as insulators for two-dimensional transistors. Nature, 2022, 605, 262-267.	13.7	109
12	Promoting visible-light photocatalytic activities for carbon nitride based 0D/2D/2D hybrid system: Beyond the conventional 4-electron mechanism. Applied Catalysis B: Environmental, 2020, 270, 118870.	10.8	107
13	Reversible Hydrophobic to Hydrophilic Transition in Graphene via Water Splitting Induced by UV Irradiation. Scientific Reports, 2014, 4, 6450.	1.6	105
14	Vanadium doped 1T MoS2 nanosheets for highly efficient electrocatalytic hydrogen evolution in both acidic and alkaline solutions. Chemical Engineering Journal, 2021, 409, 128158.	6.6	98
15	Interface-Charge Induced Giant Electrocaloric Effect in Lead Free Ferroelectric Thin-Film Bilayers. Nano Letters, 2020, 20, 1262-1271.	4.5	95
16	Electronic and magnetic properties of Co doped MoS2 monolayer. Scientific Reports, 2016, 6, 24153.	1.6	94
17	Electronic and nanostructure engineering of bifunctional MoS2 towards exceptional visible-light photocatalytic CO2 reduction and pollutant degradation. Journal of Hazardous Materials, 2020, 381, 120972.	6.5	90
18	Highly porous reticular tin–cobalt oxide composite thin film anodes for lithium ion batteries. Journal of Materials Chemistry, 2009, 19, 8360.	6.7	88

#	Article	IF	CITATIONS
19	Sb ₂ Te ₃ Nanoparticles with Enhanced Seebeck Coefficient and Low Thermal Conductivity. Chemistry of Materials, 2010, 22, 3086-3092.	3.2	83
20	Ab initio study of phase stability in doped TiO2. Computational Mechanics, 2012, 50, 185-194.	2.2	78
21	Au quantum dots engineered room temperature crystallization and magnetic anisotropy in CoFe ₂ O ₄ thin films. Nanoscale Horizons, 2019, 4, 434-444.	4.1	77
22	Functional Two-Dimensional Coordination Polymeric Layer as a Charge Barrier in Li–S Batteries. ACS Nano, 2018, 12, 836-843.	7.3	76
23	Magnetic and Conductive Liquid Metal Gels. ACS Applied Materials & Interfaces, 2020, 12, 20119-20128.	4.0	73
24	Dimensionality Controlled Octahedral Symmetry-Mismatch and Functionalities in Epitaxial LaCoO ₃ /SrTiO ₃ Heterostructures. Nano Letters, 2015, 15, 4677-4684.	4.5	71
25	Recent Progress in Lithium Lanthanum Titanate Electrolyte towards All Solid-State Lithium Ion Secondary Battery. Critical Reviews in Solid State and Materials Sciences, 2019, 44, 265-282.	6.8	69
26	Tuning catalytic performance by controlling reconstruction process in operando condition. Applied Catalysis B: Environmental, 2020, 260, 118103.	10.8	68
27	α-CsPbl ₃ Colloidal Quantum Dots: Synthesis, Photodynamics, and Photovoltaic Applications. ACS Energy Letters, 2019, 4, 1308-1320.	8.8	65
28	Heterogeneous Distribution of Sodium for High Thermoelectric Performance of pâ€ŧype Multiphase Leadâ€Chalcogenides. Advanced Energy Materials, 2015, 5, 1501047.	10.2	63
29	Ferromagnetic ordering in Mn-doped ZnO nanoparticles. Nanoscale Research Letters, 2014, 9, 625.	3.1	61
30	Nickel foam based polypyrrole–Ag composite film: a new route toward stable electrodes for supercapacitors. New Journal of Chemistry, 2013, 37, 337-341.	1.4	59
31	Improvement in the thermoelectric properties of CaMnO3 perovskites by W doping. Journal of Materials Science, 2014, 49, 7522-7528.	1.7	59
32	High-performance asymmetric supercapacitors realized by copper cobalt sulfide crumpled nanoflower and N, F co-doped hierarchical nanoporous carbon polyhedron. Journal of Power Sources, 2020, 456, 228023.	4.0	58
33	Magnetic properties in α-MnO2 doped with alkaline elements. Scientific Reports, 2015, 5, 9094.	1.6	57
34	Ultrahigh oxygen evolution reaction activity in Au doped co-based nanosheets. RSC Advances, 2022, 12, 6205-6213.	1.7	56
35	Binary Pd/amorphous-SrRuO3 hybrid film for high stability and fast activity recovery ethanol oxidation electrocatalysis. Nano Energy, 2020, 67, 104247.	8.2	55
36	FeS2 bridging function to enhance charge transfer between MoS2 and g–C3N4 for efficient hydrogen evolution reaction. Chemical Engineering Journal, 2021, 421, 127804.	6.6	51

#	Article	IF	CITATIONS
37	A Facile and Template-Free One-Pot Synthesis of Mn3O4 Nanostructures as Electrochemical Supercapacitors. Nano-Micro Letters, 2016, 8, 165-173.	14.4	50
38	Single-Crystal-like Textured Growth of CoFe ₂ O ₄ Thin Film on an Amorphous Substrate: A Self-Bilayer Approach. ACS Applied Electronic Materials, 2020, 2, 3650-3657.	2.0	49
39	Melamine Foam Derived 2H/1T MoS ₂ as Flexible Interlayer with Efficient Polysulfides Trapping and Fast Li ⁺ Diffusion to Stabilize Li–S Batteries. ACS Applied Materials & Interfaces, 2021, 13, 6229-6240.	4.0	49
40	Bifunctional water splitting enhancement by manipulating Mo-H bonding energy of transition Metal-Mo2C heterostructure catalysts. Chemical Engineering Journal, 2022, 431, 134126.	6.6	49
41	Recent Advances of Layered Thermoelectric Materials. Advanced Sustainable Systems, 2018, 2, 1800046.	2.7	47
42	Ferroelectric crystals with giant electro-optic property enabling ultracompact Q-switches. Science, 2022, 376, 371-377.	6.0	46
43	K0.25Mn2O4nanofiber microclusters as high power cathode materials for rechargeable lithium batteries. RSC Advances, 2012, 2, 1643-1649.	1.7	44
44	Zn vacancy induced ferromagnetism in K doped ZnO. Journal of Materials Chemistry C, 2015, 3, 11953-11958.	2.7	43
45	Electronic and Magnetic Properties of Transition-Metal-Doped Monolayer Black Phosphorus by Defect Engineering. Journal of Physical Chemistry C, 2016, 120, 9773-9779.	1.5	43
46	Digital to analog resistive switching transition induced by graphene buffer layer in strontium titanate based devices. Journal of Colloid and Interface Science, 2018, 512, 767-774.	5.0	43
47	From Titanium Sesquioxide to Titanium Dioxide: Oxidation-Induced Structural, Phase, and Property Evolution. Chemistry of Materials, 2018, 30, 4383-4392.	3.2	42
48	Co–Al-substituted strontium hexaferrite for rare earth free permanent magnet and microwave absorber application. Journal Physics D: Applied Physics, 2021, 54, 024001.	1.3	42
49	Nitrogen/oxygen co-doped carbon nanofoam derived from bamboo fungi for high-performance supercapacitors. Journal of Power Sources, 2020, 479, 228835.	4.0	41
50	Enhancement of the Stability of Fluorine Atoms on Defective Graphene and at Graphene/Fluorographene Interface. ACS Applied Materials & Interfaces, 2015, 7, 19659-19665.	4.0	39
51	Power Factor Enhancement for Few-Layered Graphene Films by Molecular Attachments. Journal of Physical Chemistry C, 2011, 115, 1780-1785.	1.5	38
52	Evidence of Filamentary Switching in Oxide-based Memory Devices via Weak Programming and Retention Failure Analysis. Scientific Reports, 2015, 5, 13599.	1.6	37
53	Accelerating CO2 reduction on novel double perovskite oxide with sulfur, carbon incorporation: Synergistic electronic and chemical engineering. Chemical Engineering Journal, 2022, 446, 137161.	6.6	34
	Strong Effect of Oxygen Partial Pressure on Electrical Properties of		

54 0.5Ba(Zr_{0.2}Ti_{0.8})O₃â€"0.5(Ba_{0.7}Ca_{0.3})TiO<subъĝ</sub>33</sub>33</sub>33
Thin Films. Journal of the American Ceramic Society, 2015, 98, 2094-2098.

#	Article	IF	CITATIONS
55	Ga Substitution and Oxygen Diffusion Kinetics in Ca ₃ Co ₄ O _{9+Î} -Based Thermoelectric Oxides. Journal of Physical Chemistry C, 2013, 117, 13382-13387.	1.5	32
56	Doping concentration dependence of microstructure and magnetic behaviours in Co-doped TiO2 nanorods. Nanoscale Research Letters, 2014, 9, 673.	3.1	32
57	Ethanol-directed morphological evolution of hierarchical CeO _x architectures as advanced electrochemical capacitors. Journal of Materials Chemistry A, 2015, 3, 13970-13977.	5.2	32
58	XPS study of cobalt doped TiO ₂ films prepared by pulsed laser deposition. Surface and Interface Analysis, 2014, 46, 1043-1046.	0.8	29
59	Voltage sweep modulated conductance quantization in oxide nanocomposites. Journal of Materials Chemistry C, 2014, 2, 10291-10297.	2.7	29
60	Multiple Anionic Transition-Metal Oxycarbide for Better Lithium Storage and Facilitated Multielectron Reactions. ACS Nano, 2019, 13, 11665-11675.	7.3	28
61	Large Piezoelectricity and Ferroelectricity in Mnâ€Doped (Bi _{0.5} Na _{0.5})TiO ₃ â€BaTiO ₃ Thin Film Prepared by Pulsed Laser Deposition. Journal of the American Ceramic Society, 2016, 99, 2347-2353.	1.9	27
62	Illumination-Induced Phase Segregation and Suppressed Solubility Limit in Br-Rich Mixed-Halide Inorganic Perovskites. ACS Applied Materials & Interfaces, 2020, 12, 38376-38385.	4.0	27
63	Nickel-Based Selenides with a Fractal Structure as an Excellent Bifunctional Electrocatalyst for Water Splitting. Nanomaterials, 2022, 12, 281.	1.9	27
64	Stochastic memristive nature in Co-doped CeO2 nanorod arrays. Applied Physics Letters, 2013, 103, .	1.5	26
65	Steam-Assisted Chemical Vapor Deposition of Zeolitic Imidazolate Framework. , 2020, 2, 485-491.		26
66	Zinc oxide nanotubes decorated with silver nanoparticles as an ultrasensitive substrate for surface-enhanced Raman scattering. Mikrochimica Acta, 2012, 179, 315-321.	2.5	25
67	Thermoelectric properties of Yb and Nb codoped CaMnO ₃ . Physica Status Solidi (A) Applications and Materials Science, 2014, 211, 1200-1206.	0.8	24
68	Ultralight, highly flexible and conductive carbon foams for high performance electromagnetic shielding application. Journal of Materials Science: Materials in Electronics, 2018, 29, 13643-13652.	1.1	24
69	Thermoelectric performance enhancement by manipulation of Sr/Ti doping in two sublayers of Ca3Co4O9. Journal of Advanced Ceramics, 2020, 9, 769-781.	8.9	24
70	A melt-diffusion strategy for tunable sulfur loading on CC@MoS2 for lithium–sulfurâ€< batteries. Energy Reports, 2020, 6, 172-180.	2.5	24
71	Tuneable resistive switching characteristics of In2O3 nanorods array via Co doping. RSC Advances, 2013, 3, 13422.	1.7	23
72	Periodicity Dependence of the Built-in Electric Field in (Ba _{0.7} Ca _{0.3})TiO ₃ /Ba(Zr _{0.2} Ti _{0.8})O _{3Ferroelectric Superlattices. ACS Applied Materials & Interfaces, 2015, 7, 26301-26306.}	ıb×4.0	23

#	Article	IF	CITATIONS
73	Defect engineering in perovskite oxide thin films. Chemical Communications, 2021, 57, 8402-8420.	2.2	22
74	Recent Developments in Oxide-Based Ionic Conductors: Bulk Materials, Nanoionics, and Their Memory Applications. Critical Reviews in Solid State and Materials Sciences, 2018, 43, 47-82.	6.8	20
75	Correlating the Composition-Dependent Structural and Electronic Dynamics of Inorganic Mixed Halide Perovskites. Chemistry of Materials, 2020, 32, 2470-2481.	3.2	20
76	<i>In situ</i> phase transition induced TM–MoC/Mo ₂ C (TM= Fe, Co, Ni, and Cu) heterostructure catalysts for efficient hydrogen evolution. Journal of Materials Chemistry A, 2022, 10, 10493-10502.	5.2	20
77	Manipulation of charge carrier concentration and phonon scattering via spin-entropy and size effects: Investigation of thermoelectric transport properties in La-doped Ca3Co4O9. Journal of Alloys and Compounds, 2019, 801, 60-69.	2.8	19
78	Crystallographic Orientation Dependence on Electrical Properties of (<scp><scp>Bi</scp></scp> , <scp>Na</scp> , <scp>Si</scp> Thin Films. Journal of the American Ceramic Society, 2013, 96, 3530-3535.	1.9	18
79	Interfacial Redox Reactions Associated Ionic Transport in Oxide-Based Memories. ACS Applied Materials & Interfaces, 2017, 9, 1585-1592.	4.0	17
80	Orbital engineering of two-dimensional materials with hydrogenation: A realization of giant gap and strongly correlated topological insulators. Physical Review B, 2015, 92, .	1.1	16
81	Highly Conductive PDMS Composite Mechanically Enhanced with 3D-Graphene Network for High-Performance EMI Shielding Application. Nanomaterials, 2020, 10, 768.	1.9	16
82	Manipulation of planar oxygen defect arrangements in multifunctional magnÃ"li titanium oxide hybrid systems: from energy conversion to water treatment. Energy and Environmental Science, 2020, 13, 5080-5096.	15.6	15
83	NH3-Sensing Mechanism Using Surface Acoustic Wave Sensor with AlO(OH) Film. Nanomaterials, 2019, 9, 1732.	1.9	14
84	Growth of High-Quality Monolayer Transition Metal Dichalcogenide Nanocrystals by Chemical Vapor Deposition and Their Photoluminescence and Electrocatalytic Properties. ACS Applied Materials & Interfaces, 2021, 13, 47962-47971.	4.0	14
85	Oxygen Vacancy Dependence of Magnetic Behavior in the LaAlO 3 /SrTiO 3 Heterostructures. Advanced Materials Interfaces, 2016, 3, 1600547.	1.9	13
86	UV irradiation induced reversible graphene band gap behaviors. Journal of Materials Chemistry C, 2016, 4, 8459-8465.	2.7	13
87	Tunable high acoustic impedance alumina epoxy composite matching for high frequency ultrasound transducer. Ultrasonics, 2021, 116, 106506.	2.1	13
88	Immobilization of Na Ions for Substantial Power Factor Enhancement: Site-Specific Defect Engineering in Na _{0.8} CoO ₂ . Journal of Physical Chemistry C, 2012, 116, 4324-4329.	1.5	12
89	Subtle Interplay between Localized Magnetic Moments and Itinerant Electrons in LaAIO ₃ /SrTiO ₃ Heterostructures. ACS Applied Materials & Interfaces, 2016, 8, 13630-13636.	4.0	12
90	Thermoelectric properties of sol–gel derived lanthanum titanate ceramics. RSC Advances, 2015, 5, 14735-14739.	1.7	11

#	Article	IF	CITATIONS
91	Novel synthesis and thermal property analysis of MgO–Nd2Zr2O7 composite. Ceramics International, 2016, 42, 16888-16896.	2.3	11
92	One‣tep Synthesis of N/S Codoped "Porous Carbon Cloth―as a Sulfur Carrier for Lithium–Sulfur Batteries. Energy Technology, 2020, 8, 2000188.	1.8	11
93	A comparative study of the structural and optical properties of Si-doped GaAs under different ion irradiation. Optical Materials, 2021, 111, 110611.	1.7	11
94	Superior Hydrogen Sorption Kinetics of Ti0.20Zr0.20Hf0.20Nb0.40 High-Entropy Alloy. Metals, 2021, 11, 470.	1.0	11
95	Improved super-capacitive performance of carbon foam supported CeO _x nanoflowers by selective doping and UV irradiation. RSC Advances, 2014, 4, 35067-35071.	1.7	10
96	Probing complementary memristive characteristics in oxide based memory device via non-conventional chronoamperometry approach. Applied Physics Letters, 2016, 108, 033506.	1.5	10
97	Superconductivity and structural instability in layered BiS ₂ -based LaO _{1â^'x} BiS ₂ . Journal of Materials Chemistry C, 2019, 7, 586-591.	2.7	10
98	Tunable thermopower and thermal conductivity in Lu doped In2O3. RSC Advances, 2014, 4, 31926-31931.	1.7	9
99	Bipolar resistive switching characteristics in LaTiO3 nanosheets. RSC Advances, 2014, 4, 18127.	1.7	9
100	Enhanced Photovoltaic Effect in Feâ€Doped (Bi, Na) TiO ₃ â€BaTiO ₃ Ferroelectric Ceramics. International Journal of Applied Ceramic Technology, 2016, 13, 896-903.	1.1	9
101	Sintering and electrical properties of commercial PZT powders modified through mechanochemical activation. Journal of Materials Science, 2018, 53, 13769-13778.	1.7	9
102	Microscopic investigations of switching phenomenon in memristive systems: a mini review. RSC Advances, 2018, 8, 28763-28774.	1.7	9
103	Strain-Directed Layer-By-Layer Epitaxy Toward van der Waals Homo- and Heterostructures. , 2021, 3, 442-453.		9
104	New insights on the substantially reduced bandgap of bismuth layered perovskite oxide thin films. Journal of Materials Chemistry C, 2021, 9, 3161-3170.	2.7	9
105	Multitasking Memristor for High Performance and Ultralow Power Artificial Synaptic Device Application. ACS Applied Electronic Materials, 2022, 4, 3154-3165.	2.0	9
106	Recent progress in high Bs and low Hc Fe-based nanocrystalline alloys. Nanotechnology Reviews, 2014, 3, .	2.6	8
107	Electric field manipulated reversible hydrogen storage in graphene studied by <scp>DFT</scp> calculations. Physica Status Solidi (A) Applications and Materials Science, 2014, 211, 351-356.	0.8	8
108	The effect of annealing oxygen concentration in the transformation of Ca _x CoO ₂ to thermoelectric Ca ₃ Co ₄ O ₉ . RSC Advances, 2015, 5, 28158-28162.	1.7	8

#	Article	IF	CITATIONS
109	Evidencing the existence of intrinsic half-metallicity and ferromagnetism in zigzag gallium sulfide nanoribbons. Scientific Reports, 2014, 4, 5773.	1.6	8
110	Tunable electronic and magnetic properties of arsenene nanoribbons. RSC Advances, 2017, 7, 51935-51943.	1.7	8
111	Manipulating resistive states in oxide based resistive memories through defective layers design. RSC Advances, 2017, 7, 56390-56394.	1.7	8
112	Realization of exchange bias control with manipulation of interfacial frustration in magnetic complex oxide heterostructures. Physical Review B, 2021, 104, .	1.1	8
113	An atlas of room-temperature stability and vibrational anharmonicity of cubic perovskites. Materials Horizons, 2022, 9, 1896-1910.	6.4	8
114	Size Dependence and Spatial Variation of Electronic Structure in Nonpolar ZnO Nanobelts. Journal of Physical Chemistry C, 2009, 113, 4804-4808.	1.5	7
115	Dehydrogenation: a simple route to modulate magnetism and spatial charge distribution of germanane. Journal of Materials Chemistry C, 2015, 3, 3128-3134.	2.7	7
116	Origins of possible synergistic effects in the interactions between metal atoms and MoS ₂ /graphene heterostructures for battery applications. Physical Chemistry Chemical Physics, 2018, 20, 18671-18677.	1.3	7
117	Defect induced charge trapping in C-doped α-Al2O3. Journal of Applied Physics, 2017, 122, 025702.	1.1	6
118	Thickness Dependence of Magnetic Behavior of LaAlO 3 /SrTiO 3 Heterostructures. Advanced Materials Interfaces, 2018, 5, 1800352.	1.9	6
119	Phase formation and microstructure evolution in mullite ceramics synthesized from mechanochemically activated oxide powders doped with Cr2O3. Journal of Physics and Chemistry of Solids, 2018, 123, 198-205.	1.9	5
120	The interplay among molecular structures, crystal symmetries and lattice energy landscapes revealed using unsupervised machine learning: a closer look at pyrrole azaphenacenes. CrystEngComm, 2019, 21, 6173-6185.	1.3	5
121	Atomic Stacking Configurations in Atomic Layer Deposited TiN Films. Journal of Physical Chemistry B, 2002, 106, 12797-12800.	1.2	4
122	The effects of composition deviations on the microstructure and thermoelectric performance of Ca3Co4O9 thin film. Journal of Materials Science: Materials in Electronics, 2018, 29, 13321-13327.	1.1	4
123	Enhanced Field Electron Emission Properties of Hybrid Carbon Nanotubes Synthesized by RFâ€PECVD. Chemical Vapor Deposition, 2009, 15, 291-295.	1.4	3
124	Glassy Magnetic Transitions and Accurate Estimation of Magnetocaloric Effect in Ni–Mn Heusler Alloys. ACS Applied Materials & Interfaces, 2020, 12, 43646-43652.	4.0	3
125	Oxygen Migration in Dense Spark Plasma Sintered Aluminumâ€Doped Neodymium Silicate Apatite Electrolytes. Journal of the American Ceramic Society, 2013, 96, 3457-3462.	1.9	2

126 Magnetic Nanomaterials for Electromagnetic Wave Absorption. , 2017, , 473-514.

2

#	Article	IF	CITATIONS
127	Improved densification and thermoelectric performance of In5SnSbO12 via Ga doping. Journal of Materials Science, 2018, 53, 6741-6751.	1.7	2
128	Probing the Origin of Gold Dissolution and Tunneling Across Ni ₂ P Shell Using in situ Transmission Electron Microscopy. ACS Applied Materials & Interfaces, 2019, 11, 46947-46952.	4.0	2
129	Can Metal Intermixing Cooperatively Improve Perovskites as Redox Materials for Thermochemical Ammonia Synthesis? A Case Study on (Sr,Y)(Ti,Ru)O ₃ . Journal of Physical Chemistry C, 2021, 125, 17019-17030.	1.5	2
130	Insight into the growth behaviors of MoS2 nanograins influenced by step edges and atomic structure of the substrate. Nano Research, 2022, 15, 7646-7654.	5.8	2
131	Giant stability of substituent Co chains in ZnO:Co dilute magnetic oxides. AlP Advances, 2012, 2, 042155.	0.6	1
132	Phononic Structure Engineering: the Realization of Einstein Rattling in Calcium Cobaltate for the Suppression of Thermal Conductivity. Scientific Reports, 2016, 6, 30530.	1.6	1
133	Effect of the geometry of precursor crucibles on the growth of MoS ₂ flakes by chemical vapor deposition. New Journal of Chemistry, 2020, 44, 21076-21084.	1.4	1
134	Microtexture Mapping of Elecrtron Backscattered Diffraction in (Bi,Pb)2Sr2Ca2Cu3O10 Superconductor Tapes. Materials Research Society Symposia Proceedings, 2000, 659, 1.	0.1	0
135	The magnetism of BiFeO ₃ powders. Functional Materials Letters, 2015, 08, 1550027.	0.7	Ο